Measurement and Modelling of the Propagation Channel between Low Height Terminals

Konstantinos Konstantinou, Shaoli Kang, Tim Brown and Costas Tzaras

Abstract

The evaluation of communication systems with low-height terminals requires path loss models that are applicable to low-height links. For the terminology low-height, the range 0.5 (mobile-) to 3m (fixed-node) above ground is considered. Herein, empirical non-time-dispersive propagation models for relaying systems with low-height terminals are proposed. The models consist of line-of-sight and non-line-of-sight branches. Single- and two-slope modelling approaches were examined. The models take into account the effect of frequency, transmitter and receiver height, and environment. They are complemented by shadowing and fast-fading distribution and correlation statistics. The performance of the models in producing accurate estimations is evaluated by comparison with sets of independent data.

Index Terms

Path Loss, LOS, NLOS, Shadowing, Fading, Relay, Low Height Terminal.

I. Introduction

The reliability and multiple functionalities of mobile devices are broadly considered the main reasons for the great mobile communications penetration in the population. As the number of subscribers and their demands in services rise the mobile systems are confronted with the underlying medium capacity- and coverage-limits. The multihop (relaying) technology is thought of as an alleviating technique to subdue the severity of these restrictions.

It has been well-accepted that the use of accurate propagation models between the relay and relayee is of greatest importance. The correct evaluation of a relaying system's performance requires a suitable propagation model and hence studying this effect is the motivating force for this research. Relaying is a potential enhancement of systems which operate in different spectrum ranges, such as GSM, UMTS, LTE, and LTE Advanced. The wide range of frequencies used by

wireless sensor networks and cognitive radio technology all support the motive for studying the propagation channel over a broader frequency range.

The literature offers several signal power-level prediction-techniques to estimate the local average value, slow fading and time-dispersion parameters. Aware of the importance in studying the low-height communication-link propagation-characteristics, research has produced several empirical models [1]–[9]. Single-slope [1]–[3], [5], [6], [9], [10], two-slope [8], [11], and even three-slope [4] models have been proposed, which consider heights compatible with the low-height channel of this study. In [12], measurements were conducted, at a very near to the ground level (receiver height at 3 to 28cm), at 880MHz, in an urban environment. In addition, organisations and industry have also undertaken research in the field. ITU [11] introduced separate path loss models for Line-Of-Sight (LOS) and Non-LOS (NLOS) links, with the transmitter situated below the rooftop level. WINNER [13] produced reports on indoor and outdoor LOS measurements. COST231 [14] suggests a modification on the well-known Hata model, for urban areas. There is a lack of propagation models which cover the system parameter-ranges that relaying networks will be operating in: frequency, separation distance and terminal-height ranges, and environments. Consolidating the problem, in order to perform a quality analysis of the relaying applicability and to quantify its benefits of its employment a suitable path loss model is required.

In this paper we establish a measurement-based prediction model, which is valid for transceiver antennas between the very-near-to-ground and street-lamp levels. Although limited, the peer-to-peer links of ad hoc systems in an urban and suburban environment are to take place in this height range. Our investigation did not extend to greater heights due to them being covered satisfactorily by literature models. The model was founded by a measurement campaign which covered various frequencies, transmitter and receiver heights, and environments.

Regression analysis was used to extract the model terms and coefficients. The accuracy in estimating the path loss of the models was tested against independent data sets. Analyses of shadow fading and fast fading are also provided as an accompaniment to the proposed models.

The remainder of the paper is organised as follows: In Section II, the measurement campaign is described. In Section III the measurement-data pre-processing and regression-strategy are analysed. The literature models' applicability at low height channels is examined. In Section IV, empirical path loss models are proposed for LOS and NLOS links. The shadow- and fast-fading

statistics are analysed in Sections V and VI, respectively. Conclusions are drawn in the final section.

II. Description of the Measurement Process

In our endeavour to cover different real urban morphology scenarios, we used a UK Geographic Information System (GIS) database to assess information on the building, vegetation (parks), and water (river, canals) block edges, amongst others. Other provided information was the ground and building height, and coordinates of the central line of each street. We specified two areas for the measurement campaign: London was selected as a representative of a highly urbanised environment, whereas, Reading as an example of a typical suburban-morphology. The areas selection (see Fig. 1) was based on the average characteristics of: the building and vegetation height and density, road width and percentage of LOS locations given the transmitter position. The large number of measurement runs and locations provided with repeatability and diversity of environment. The great-quantity of data-points for each frequency, antenna-height configuration, and environment, aided the discernability of each factor's effect on the mean path loss function.

During the campaign the received power of different paths was recorded in a simultaneous manner. To specify the waveform of the channel-sounding signal, the transmitter sources were used in continuous wave mode (i.e. sinusoidal wave, no data were transmitted). The following frequencies were used: 420MHz (fL) corresponding to the terrestrial trunked radio, 935MHz (fM) representing the GSM or UMTS at 900MHz system and 2020MHz (fH) corresponding to the UMTS and extrapolatingly the wireless local area network 802.11g; see Fig. 2.

The transmitter antennas were three half wave-length vertical-polarised omnidirectional dipoles, one for each frequency, and with a 2dBi gain. Their height, which was equal among themselves and fixed throughout the measurement run, was alternated between 1.8 ("L", human node or a handheld device) and 3m ("H", pole node) in each run/location. Several runs per location were conducted to sample adequately both heights. The $\mathrm{EIRP} \in (41.7,\ 44.4)$dBm, which was dependent on the carrier frequency f_{c}, was measured before each measurement run.

Six narrowband-mode receivers (7.5kHz) recorded the power of six paths: the combination of the three transmit frequencies, each received at two fixed height-levels, 1.8m ("L") and 3m ("H") , as summarised in Table I. Unlike in the transmitting end the recording at the two receiver heights was performed in a simultaneous manner. The receiver antennas were six half-wavelength

vertical-polarised omnidirectional dipoles, two for each measured $f_{\rm c}$, and with a $G_{\rm R} = 2$dBi gain.

All antennas were placed upright (no mechanical down-tilt). The position of the transmitter (receiver) antenna and cabling to the transmitter (receiver) hardware was secured with sticky-tape onto a tripod (the vehicle-body). The transmitters and receivers were calibrated by the manufacturer on a yearly basis. Additionally before the measurements: the transmitter output was measured with a spectrum analyser, the receiver offset was calculated by measuring the recorded power at the receiver for a known input signal, and the connectors were tested. A test measurement was conducted inside an anechoic chamber and the recordings were compared to the free-space-loss predictions.

During each measurement run, the transmitters were stationary, while a vehicle bearing the receiving equipment was covering all streets around the transmitters fixed-location. Each receiver had a sensitivity of about -120dBm. Software dynamically adjusted a pad attenuator at the receiver end. A wheel-attached odometer provided the distance triggering to record the power-level, taken at 100kHz bursts (time-), every λ/5 (distance-resolution), where λ the carrier wavelength. The distance- and time-resolution suffices for examination of both large- and small-scale components (small-scale variations are experienced in $\lambda/2$). Each location-point was tagged with a time and Global Positioning System (GPS) location-stamp. The antennas were separated horizontally by an invariable distance that was greater than 1.5m, which is greater than the minimum $\lambda/2$ of the measurement frequencies. As a rule of thumb a greater than $\lambda/2$ antenna separation is required to avoid mutual-coupling.

The non-ideal radiation patterns degraded the accuracy of the measurements which cannot be compensated for without knowledge of the angle of arrival. However, the induced error can be reduced by repetition of the measurement route in the opposite direction. Close to the transmitter, the direct path prevails and the recorded received signal is expected to deviate due to elevation spread.

III. Data Pre-Processing

In this section the measurement-data pre-processing is discussed, a comparison of the measurement-data against the predictions of the most widely-used models is conducted and the regression analysis technique that is used to develop the empirical propagation model is presented.

A. Data Pre-Processing

The widely used Lee sampling criterion [7] for uncorrelated samples was employed, succeeded by a graphical verification of the fast fading component removal. Due to sky obstruction from buildings, the GPS accuracy was jeopardised and some recorded positions faced a drift from their actual locations. We assumed that when the vehicle was at standstill the GPS tag was exempt from error. For each interim travelled segment we relocated the erroneous points by equidistant placement along the travelled trajectory, which was applicable due to the distance triggering nature of the measurements. The GIS database and satellite imaging facilitated the relocation. Note that the location data are used to calculate the distance from the transmitter, which participates in the propagation formulas in the logarithmic scale. Thus the induced error caused by the GPS position drift is expected to be suppressed.

Prior to the recordings an area scanning was performed for possible interfering signals to determine the existence of alien sources. After the campaign completion, the power in each receiver was examined for abnormal values in comparison to the recorded data at the other recorded frequencies. Additionally, the recorded received power was compared to the anticipated received power level due to the free space loss. For that, the LOS property of each recorded location, which was verified cartographically from the GIS database, was taken into consideration.

Measurement-points lying behind vegetation- or water-areas were excluded from the mean path loss formulation process. These points appeared as outliers and reduced the effectiveness of minimising the mean path loss model error. It is noted that among the possible foliage types, only parks are herein characterised as vegetation areas, whereas data-points behind gardens, hedges, etc. were included in the regression analysis. This was because the GIS foliage database provided details only on the park clutter. The number of measurement data-points behind vegetation was not adequate so as to perform statistics in order to potentially derive foliage calibration factors. It is noted however that these excluded points were taken into account at the shadowing modelling.

The path loss values L were calculated by recording the local mean power P_{R}, by:

$$L = \mathrm{EIRP} + G_{\mathrm{R}} - L_{\mathrm{R}} - P_{\mathrm{R}} \tag{1}$$

where L_{R} is the receiver offset and cable loss [$L_{\mathrm{R}} \in (0.74,\ 2.25)\mathrm{dB}$, depending on the frequency]. All variables are expressed in decibels. Note that both transmitter- (implicitly) and

receiver- (explicitly) antenna heights are included in the above definition and measurement of the path loss.

B. Comparison of Measurement Data with Existing Models

In existing literature, non-time-dispersive empirical propagation models which are extensively used in network planning are: the ITUR [11], the COST231-Hata [14] and the WINNER II [13]. These models' mean path loss predictions deviate from the recorded values of the measurement campaign. If the above models were employed, then their performance statistics would have been: COST231-Hata ($\mathrm{ME} = 5.22$dB, $\mathrm{RMSE} = 12.5$dB), ITUR ($\mathrm{ME} = -5.40$dB, $\mathrm{RMSE} = 11.7$dB), and WINNER II ($\mathrm{ME} = 11.0$dB, $\mathrm{RMSE} = 24.1$dB). ME is the mean error and RMSE is the root mean squared error. The performance of the proposed models is provided in Section IV B.

C. Analysis Strategy

The developed model is required to fill in the antenna-height gap, which is left out of the applicability range of its counterparts, and, therefore, re-evaluation of the effect of the different variables is required. The parametric empirical models were derived by regression estimates of the parameters (frequency, distance, heights, environment) from the data, so that the model parameters were calibrated to reflect the data-points' response. Linear and nonlinear regression analyses were used for single- and two-slope fitting to the data, respectively. The regression analysis to the single-slope model was easily performed by converting the model to a multi-linear form. In the two-slope model, a similar conversion to a multi-linear form is also possible, provided that the regression analysis is performed on either side of the breakpoint distance x_{b}, separately, where the sole coefficient to be estimated is the second slope coefficient. Thus, the second-slope curve-fitting can be conceived as a linear regression excluding the constant term, so as to maintain the function continuity. However, the execution of the regression analyses separately, and more specifically the dependence of the second slope constant-term from the first slope, causes uncertainty on the credibility of the result being the best-fit. Thus, two-slope modelling was performed only with non-linear regression methods.

The selection of the regression-analysis predictor-terms was made so as to include the terms appearing in the literature models. Terms which considered the effective road height h_0 were also

included. Seeking the best fit iterations with different h_0 were tried. In the nonlinear two-slope fitting the coefficients on either side of the x_b were disengaged and considered independently.

In both linear and nonlinear regression analyses a backward stepwise robust regression was used. The method started with several candidate terms and performed data fitting to the model. In succession, it tested the terms for statistical significance, calculated the fitting coefficients' confidence bounds and deleted insignificant terms from the model. The method also deleted the terms with great confidence bounds. The rejection of the model terms due to insignificance (exit tolerance 0.10) is based on the hypothesis test of the term to have a zero coefficient. The threshold for rejection of the model terms due to them having great confidence bounds was loosely set, nevertheless, overfitting was scarcely found during the analyses because of the large volume of recorded data-points. Readmission of the excluded terms to the model was not permitted.

In order to avoid the effect of outliers, iteratively re-weighted least-squares with a selected weighting function was performed. The following functions were tried: bisquare, logistic, andrews, cauchy, fair, huber, talwar, and welsch. The most popular weighting function is the bisquare, which has a dramatic change in weighting among the data that may be responsible for unsuccessful regression due to being biased to one or more specific measurement scenarios (antenna height and frequency configurations). The errors' minimisation determine the model coefficients thus the uneven volume of measurement points in each scenario maps to biased curve fitting. Consideration of drastically changing weighting functions such as the bisquare minimises artificially the residuals, and the derived best-fit model fails to perform well in all scenarios.

The best performing weighting function was sought before the initiation of each regression. The selection was based on the function performance in regressing a known synthetic shadowing model. Ordinary-least-squares was found to perform best and was selected in all analyses.

IV. Mean Path Loss Models

In the presented models, the involved heights and distances (fixed node- h_B, mobile node- h_M, effective road-height h_0, separation- d, breakpoint-distance x_b) are expressed in metres, carrier frequency f_c in MHz, and path loss estimation L in decibels. The variable scopes are: $f_\mathrm{c} \in (420,\ 2020)$MHz, $1.8 < \{h_\mathrm{B}, h_\mathrm{M}\} < 3.0$m, and $d < 250$m (LOS) or $d < 5000$m (NLOS). Note that the predictions are for the average path loss and that fades related to the channel frequency response were not modelled.

A. LOS (single- and two-slope) and NLOS Proposed Models

With respect to the single-slope LOS model:

$$L = 29.0 + f \log f_{\rm c} + 10n \log d - 194 \log h_{\rm M} + C \tag{2}$$

where $\log$ denotes the logarithm on base 10, $n = 3.16 - 2.15 \log h_{\rm B}$, $f = 63.3 \log h_{\rm M}$, and $C = 4.13$dB (dense urban) or 0.97 (suburban or urban). Based on conditions:

1) The path-loss slope-coefficient $n \in (2.17,\ 2.51)$ is a negatively proportional function of the fixed node height $h_{\rm B}$. The range is suggestive of the data-points lying entirely on the first slope of a two-slope model. This argument is supported by the slope-coefficient n lying within the ITUR LOS first-slope bounds, also matching WINNER II LOS (first-slope).
2) The environmental effect C is an explicit calibration parameter, suggesting an additional path loss of 3.16dB in the dense urban case, in good agreement with COST231-Hata model.
3) The frequency-term coefficient $f \in (19.1,\ 29.3)$dB, is in good agreement with [1], [2], [5], [6]. The coefficient f is proportional to $\log h_{\rm M}$, the mobile node height in logarithmic scale. Dependence of the coefficient f on the mobile node height $h_{\rm M}$ can be found in [14].
4) Apart from the effect on the slope- n and the frequency-coefficient f, the transceiver heights contribute to the path-loss estimation explicitly. This model suggests an additional path loss of 31.3dB for a 0.9m drop in the mobile terminal height, similar to [12].

Scatter-plots of the LOS measurement points and the proposed model single-slope predictions are plotted in Fig. 3. Each line corresponds to a frequency and height configuration, which displaces the function on the y-axis and changes its slope. The predicted path loss lines alternate between an upper and a lower curve. This was done to show the alternation due to the environmental effect. For best visibility only the high- and low-frequency are plotted, and the x-axis is limited to 200m, and the path gain values are plotted instead of the path loss. The model agrees well with [1], [2], [6], [8], [9], [11], [13].

With respect to the two-slope LOS model:

$$L = -77.6 + \begin{cases} 10n_1 \log d + 40.9 \log f_{\rm c} & \text{, if } d < x_{\rm b} \\ 10n_1 \log x_{\rm b} + 10n_2 \log \frac{d}{x_{\rm b}} + 39.6 \log f_{\rm c} + C & \text{, if } d \geq x_{\rm b} \end{cases} \tag{3}$$

where $n_1 = 0.817 + 0.842\log(h_{\rm M} - h_0)$, $n_2 = 3.08 - 1.23\log(h_{\rm B} - h_0)$, $x_{\rm b} = \frac{4}{\lambda}(h_{\rm B} - h_0)(h_{\rm M} - h_0)$, $h_0 = 0.861$m, and $C = 4.63$dB (dense urban) or $C = 1.09$dB (suburban or urban). Based on conditions:

1) The effective road height h_0 and consequently the break-point distance $x_{\rm b}$ lie close to that of [13]. The best-fit in the single-slope expression was $h_0 = 0$, so that its effect was cancelled. Contrariwise, eqn. (3) defines the $x_{\rm b}$ and participates in the path-loss model-terms. The breakpoint $x_{\rm b} \in (8,\ 111)$m depending on the height configuration and carrier frequency $f_{\rm c}$.
2) The path-loss slope-coefficient n is made dependent on the terminal heights, at either side of the breakpoint distance $x_{\rm b}$. This dependence, however, exists only for $d > x_{\rm b}$. At short distances ($d < x_{\rm b}$, $n = n_1$) $n \in (0.865,\ 1.08)$ matching the high transmitter height slope-coefficient of [8] and close to the first slope of the two-slope regression fit of [4]. The mean path loss slope coefficient is expected to assume a value that is less than 2, according to the wave-guiding property that characterises this type of environment [15]. At further distances ($d \geq x_{\rm b}$, $n = n_2$) $n \in (2.70,\ 3.01)$ and is a function of linear proportionality with the effective mobile node height $\log(h_{\rm M} - h_0)$ in the logarithmic scale. Yet, it is higher than in the the single-slope expression.
3) Path loss dependence on the environment is not statistically significant for $d < x_{\rm b}$, because of the prevailing direct transmission path. Adversely, beyond ($d > x_{\rm b}$), a 3.54dB signal strength drop is suggested for dense urban environments, as in COST231-Hata.

The suggested two-slope LOS expression agrees well with other two-slope models: ITUR LOS mean between the upper and lower limits, WINNER II LOS, ETSI Berg, and [8].

With respect to the NLOS model:

$$L = -80.9 + f\log f_{\rm c} + 10n\log d + 107\log h_{\rm B} - 43.4\log h_{\rm M} + C \tag{4}$$

where $f = 29.8 - 15.5\log h_{\rm B} + 6.12\log h_{\rm M}$, $n = (4.54 - 2.66\log h_{\rm B} + 0.954\log h_{\rm M})$, and $C = 3.44$dB (dense urban) or $C = 0.809$dB (suburban or urban). Based on conditions:

1) The path-loss slope-coefficient n is a function of the terminal heights, in the logarithmic scale. For the considered terminal heights $n \in (3.02,\ 4.18)$, is distinctly higher than the LOS branches and practically matches the suggested values from [2], [6], [9].

2) The frequency-term coefficient $f \in (24.5,\ 28.0)$ and is a function of the terminal heights.
3) The terminal heights calibrate the path-loss explicitly $(12.1,\ 36.4)$dB. The effect of mobile node height is weaker than that of the fixed node height, as in [6], [8], [14].
4) The environment (2.63dB additional path loss) is a calibration parameter, as in [14].

The suggested NLOS model is in good agreement with other NLOS single- [6], [14] and two-slope [8], [11] models. Fig. **??** plots the scatter-plots of the NLOS measurements and several predictions of the proposed NLOS model corresponding to different frequency and antenna height configurations, as presented in Section II. For visibility only the fH and fL are plotted. Note that the path gain values are plotted instead of the path loss. In NLOS, the slope coefficient variability with the distance was examined. Two-slope modelling attempt was conducted, with a variable breakpoint distance across the measured range. However, there was no clear case of a two-slope model providing a better fit to the data, compared to that of the single-slope. Therefore, the best fit to the NLOS measurement data is the single-slope model (4).

B. Models' Performance Evaluation

Due to the outlier elimination, the weighting function and the exclusion of points behind vegetation and water only a fraction of the recorded data-points was used to "shape" the path loss models. In this subsection all recorded data-points are considered. The model performance can be tested by either: all recorded data-points, or the data-points from the independent campaign [6].

When using the same data-points, the error is confined within a $\pm$5dB range. The error standard deviation ranges from few to 10dB for most locations, receivers and models. When tested with the other campaign data-points, the error is provided for the LOS and NLOS cases, severally and jointly. With the single-slope LOS model: $\mathrm{ME} = 4.93$dB and $\mathrm{RMSE} = 15.2$dB. With the two-slope LOS model: $\mathrm{ME} = 0.153$dB and $\mathrm{RMSE} = 7.60$dB. With the NLOS model: $\mathrm{ME} = 4.24$dB and $\mathrm{RMSE} = 12.0$dB. For the aggregate of LOS and NLOS points: $\mathrm{ME} = 4.47$dB and $\mathrm{RMSE} = 13.1$dB.

V. SHADOW FADING

In our endeavour to examine if the shadow component originated from a normal distribution, the Lilliefors goodness-of-fit test [16] was used. The data-points were grouped according to their distance and scenario. Within LOS and separation distance $d \in (80,\ 100)$m, two groups

were identified, where the shadowing Standard Deviation (SD) was calculated at: $\sigma_{\rm LOS} = 11.4$dB (first-), and 12.6dB (second-group). The great LOS SD values are justified at the end of Section II.

In NLOS, the shadowing SD was calculated for 407 groups: $\sigma_{\rm NLOS} = 7.48{\rm dB}(\pm 20\%)$, in good agreement with [17]. The large number of groups permitted regression-analysis to the variable $\sigma_{\rm NLOS}$ (predictor terms: frequency, urbanisation factor, distance and antenna height). The output of this regression indicated that the variable $\sigma_{\rm NLOS}$ is dependent on these predictor terms. However, this dependence was not statistically significant and therefore not presented.

The empirical CDF of the LOS data was tested against the Extreme Value distribution: $F_X(x) = e^{-\left(1+\xi\frac{x-\mu}{\sigma}\right)^{-1/\xi}}$. The best-fit parameters with the Maximum Likelihood Estimation (MLE) were: location $\mu = -0.507$dB, scale $\sigma = 13.0$dB and shape $\xi = -2.88$. Routes of equidistant measurement-points were selected to calculate the autocorrelation. The exponentially evanescent function is typically used for modelling the autocorrelation curve [17]. Within LOS (NLOS), the de-correlation distance was calculated at 29(51)m, urban, and 26(56)m, suburban.

VI. Small Scale Fading

In the previous sections, the measurement-data were sampled with the Lee criterion, so as to average out the fast fading signal component. Herein in-depth statistics of the fast fading are presented. The Doppler spread effect is neglectable for the slow speed of the measurement vehicle. The equipment used in the measurement campaign was not appropriate for recognising the signal angle of arrival. Therefore, only the received power was recorded and the fast fading study concludes with the signal envelope modelling. Data-points for the fast fading examination were available for analysis from a single measurement run (one antenna height, frequency, and environment scenario).

Various distributions were tried (Rayleigh, Rice, Nakagami, Weibull, and Normal amongst others) separately for LOS and NLOS. The best-fit parameters were calculated by the MLE. The fading signal-amplitude was isolated from the large scale and mean path-loss variations. Due to the acquisition of measurement data in time-bursts, the empirical CDF of the derived fading amplitude values (in dBV) was estimated for each data-burst; see time-resolution in Section II. During each burst the vehicle can be assumed to be stationary. Since the fading-amplitude data-points were in the logarithmic scale, the models were also transformed to the log-scale.

Within LOS the fading followed Rician distribution; see Fig. 5. The measured data are also

plotted for comparison purposes along with the Nakagami fit. The Rician distribution was found to be suitable for all the surveyed distances. For NLOS, a wider fading-value spread is featured; see Fig. 5. The Nakagami fit was found to surpass all other studied distributions for the surveyed distance ranges. The parameters of the three distributions that fit best to the fast fading data in LOS, in NLOS, and in LOS & NLOS conditions are summarised in Table II. Almost all values of the Rician factor K were above 0dB. This maps to both LOS and NLOS fading data being better described by the Rician distribution function. The results agree well with [18].

VII. Conclusion

The received power at various positions, the map-locations of said positions, the transmitter power and its map-location were recorded in a measurement campaign, aiming at producing empirical models for antenna heights that are not thoroughly covered in literature. A synthetic shadowing channel was employed to predict the path loss and test several weighting functions. A comparison of the measurement-data against the predictions by employing the most widely-used models was also conducted, showing that some modification is required for the street-level height.

The regression-analysis models were formed of different expressions within LOS and NLOS. The LOS (NLOS) data were best-fit with a two-slope (single-slope) expression. Frequency and transceiver heights were found to be statistically important. The environment was accounted for explicitly, by means of a calibration factor. The suggested models were tested with the data-points of an independent campaign. The average error for the single-slope LOS model was found to be as little as 0.153dB. Shadowing distribution was compared to the extreme value and normal fits. The shadowing de-correlation distance was calculated. The distributions that best fit to the recorded fast fading component were the Rician (LOS) and Nakagami (NLOS).

Acknowledgment

This paper uses the OFCOM project “Predicting path loss of low-height terminals’ data. The authors would like to thank Dr Bachir Belloul for supplying the rich measurement data.

References

[1] Z. Wang, E. K. Tameh, and A. R. Nix, “Statistical peer-to-peer channel models for outdoor urban environments at 2 GHz and 5 GHz,” *IEEE 60th VTC*, vol. 7, pp. 5101–5, 26-29 Sep 2004.

[2] D. B. Green and A. S. Obaidat, “An accurate line of sight propagation performance model for ad-hoc 802.11 wireless LAN (WLAN) devices,” *IEEE ICC*, vol. 5, pp. 3424–8, 2002.

[3] H. Masui, T. Kobayashi, and M. Akaike, “Microwave path-loss modeling in urban line-of-sight environments,” *IEEE Journal on Selected Areas in Commun.*, vol. 20, no. 6, pp. 1151–5, Aug 2002.

[4] A. Tang, J. Sun, and K. Gong, “Mobile propagation loss with a low base station antenna for NLOS street microcells in urban area,” *IEEE VTS 53rd VTC*, vol. 1, pp. 333–6, 2001.

[5] N. Patwari, G. D. Durgin, T. S. Rappaport, and R. J. Boyle, “Peer-to-peer low antenna outdoor radio wave propagation at 1.8 GHz,” *IEEE 49th VTC*, vol. 1, pp. 371–5, Jul 1999.

[6] K. Konstantinou, S. Kang, and C. Tzaras, “A measurement-based model for mobile-to-mobile UMTS links,” *IEEE 65th VTC*, pp. 529–33, 22-25 Apr 2007.

[7] W. Lee, *Mobile Communications Design Fundamentals*. Indianapolis, Indiana: Howard W. Sams Co., 1986.

[8] D. Har, H. H. Xia, and H. L. Bertoni, “Path-loss prediction model for microcells,” *IEEE Trans. on Vehicular Technology*, vol. 48, no. 5, pp. 1453–62, Sep 1999.

[9] N. Papadakis, A. G. Kanatas, and P. Constantinou, “Microcellular propagation measurements and simulation at 1.8 GHz in urban radio environment,” *IEEE Trans. on Vehicular Technology*, vol. 47, no. 3, pp. 1012–26, Aug 1998.

[10] K. Sakawa, H. Masui, M. Ishii, H. Shimizu, and T. Kobayashi, “Microwave propagation characteristics depending on base-station antenna height in an urban area,” *IEEE AP-S International Symposium*, vol. 2, pp. 174–7, 2001.

[11] R. ITU-R, “Propagation data and prediction methods for the planning of short-range outdoor radiocommunication systems and radio local area networks in the frequency range 300MHz and 100GHz,” Tech. Rep.

[12] T. B. Welch, J. R. Wood, R. W. McParlin, L. K. Schulze, T. P. Flaherty, S. G. Carlone Hanson, R. J. Cahill, and R. A. Foran, “Very near ground RF propagation measurements for wireless systems,” *IEEE 51st VTC*, vol. 3, pp. 2556–8, 2000.

[13] IST-4-027756, “WINNER II channel models,” Tech. Rep., Nov 2007.

[14] “COST 231, digital mobile radio towards future generation systems,” Final report, Tech. Rep., www.lx.it.pt/cost231/final_report.htm.

[15] N. Blaunstein, “Average field attenuation in the nonregular impedance street waveguide,” *IEEE Trans. on Antennas and Propagation*, vol. 46, no. 12, pp. 1782–9, 1998.

[16] H. W. Lilliefors, “On the Kolmogorov-Smirnov test for normality with mean and variance unknown,” *Journal of the American Statistical Association*, vol. 62, p. 399402, 1967.

[17] S. R. Saunders and S. R. Simon, *Antennas and Propagation for Wireless Commun. Systems*. New York, NY, USA: John Wiley Sons, Inc., 1999.

[18] IST-2003-507581 WINNER, “Final report on link level and system level channel models,” Tech. Rep., Sep. 2003.

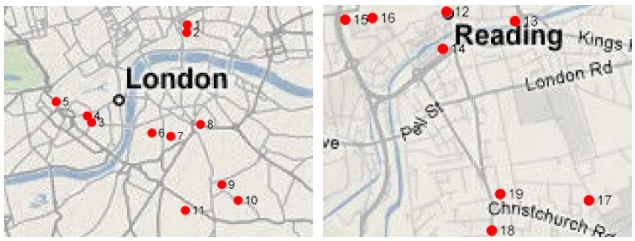

Fig. 1. Overview maps of the measurement campaign locations.

TABLE I
DESCRIPTION OF THE RECEIVING END.

	Rx 1	Rx 2	Rx 3	Rx 4	Rx 5	Rx 6
f_c [MHz]	420	420	935	935	2020	2020
Alt [m]	1.8	3	1.8	3	1.8	3

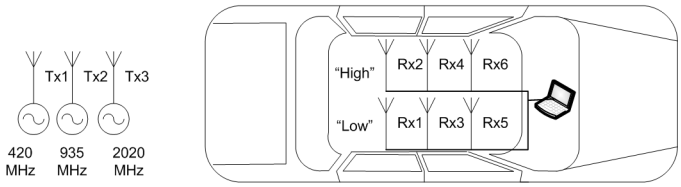

Fig. 2. Measurement equipment configuration.

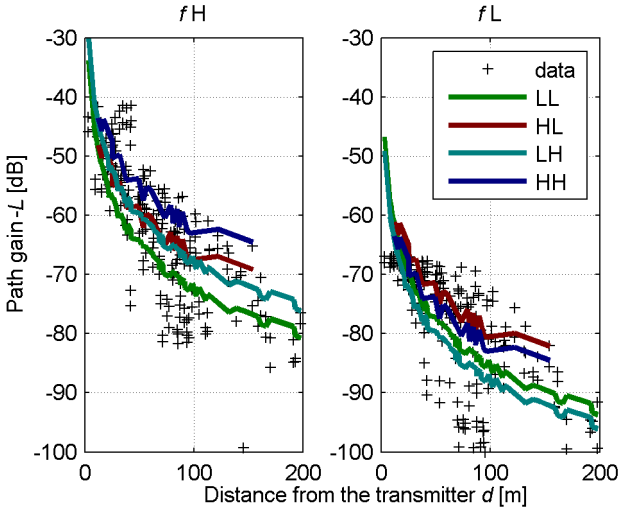

Fig. 3. "L"=1.8m, "H"=3m. Scatter-plot of the LOS measurement points and the proposed single-slope model predictions.

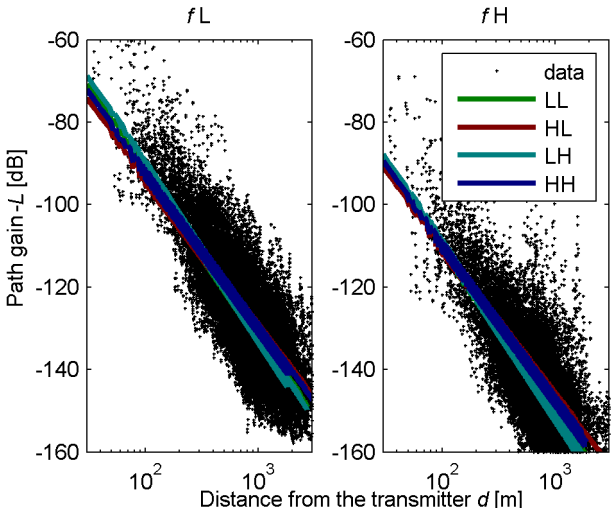

Fig. 4. "L"=1.8m, "H"=3m. Scatter-plot of the NLOS measurement points and the proposed model predictions.

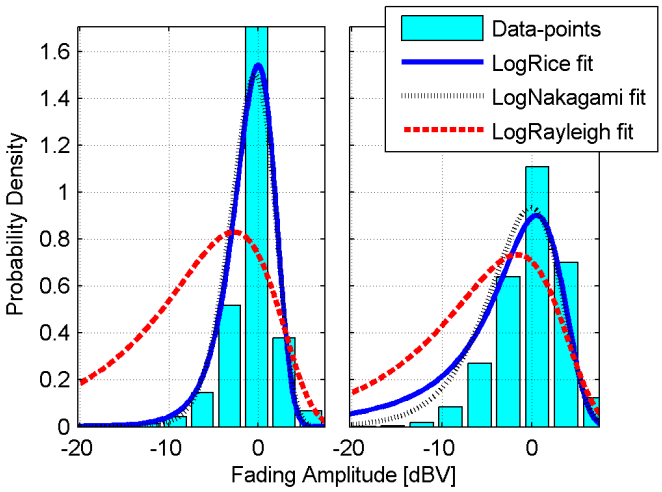

Fig. 5. Fading envelope PDF for LOS (left-) and NLOS (right-subplot). X-axis in logarithmic scale, small-scale fading amplitude expressed in dBV, and plotted distribution curves correspond to Log-Rice, Log-Nakagami, and Log-Rayleigh. The PDF curves have total area under the curves equal to 1 when the x-axis is in linear scale.

TABLE II
DISTRIBUTION PARAMETERS THAT FIT BEST TO THE FADING-AMPLITUDE.

Distribution	Fit	Rice	Nakagami	Rayleigh
LOS	coeff	$K = 12.6$dB	$m = 18.5$dB $\Omega = 1.04\text{dB}^2$	$\sigma = 0.722$dB
	RMSE	0.187	0.222	0.487
NLOS	coeff	$K = 4.17$dB	$m = 3.03$dB $\Omega = 1.11\text{dB}^2$	$\sigma = 0.745$dB
	RMSE	0.036	0.014	0.128
LOS & NLOS	coeff	$K = 9.03$dB	$m = 3.34$dB $\Omega = 0.96\text{dB}^2$	$\sigma = 0.692$dB
	RMSE	0.112	0.013	0.328